View metadata, citation and similar papers at core.ac.uk

brought to you by CORE

provided by NASA Technical Reports Server

N94-16508

A Simulation Study of the Performance of the NASA (2,1,6) Convolutional Code on RFI/Burst Channels *

Lance C. Perez
Daniel J. Costello, Jr.

Department of Electrical Engineering
University of Notre Dame
Notre Dame, Indiana 46556

October 14, 1993

*This work was supported by NASA Grants NAG5-557 and NGT-70109.

1 Introduction

In an earlier report [1], the LINKABIT Corporation studied the performance of the (2,1,6) convolutional code on the radio frequency interference (RFI)/burst channel using analytical methods. Using an R_0 analysis, the report concluded that channel interleaving was essential to achieving reliable performance. In this report, Monte Carlo simulation techniques are used to study the performance of the (2,1,6) convolutional code on the RFI/burst channel in more depth.

The basic system model under consideration is shown in Figure 1. The (2,1,6) convolutional code is the NASA standard code with generators

$$\begin{aligned} g^1 &= 1 + D^2 + D^3 + D^5 + D^6 \\ g^2 &= 1 + D + D^2 + D^3 + D^6 \end{aligned}$$

and $d_{free} = 10$. The channel interleaver is of the convolutional or periodic type first described in [2]. The binary output of the channel interleaver is transmitted across the channel using binary phase shift keying (BPSK) modulation. The transmitted symbols are corrupted by an RFI/burst channel consisting of a combination of additive white Gaussian noise (AWGN) and RFI pulses. At the receiver, a soft-decision Viterbi decoder with no quantization and variable truncation length is used to decode the deinterleaved sequence.

2 RFI Channel Models

The RFI/burst channel takes on a variety of forms depending on the characteristics of the RFI pulse and the steps taken to combat it. In this report, the two models described in [1] are used. These models represent the two extremes of the RFI/burst channel.

In the first model, the RFI pulse is assumed to saturate the satellite's transponder to the extent that BPSK symbols at the output of the channel occur with equal probability during the RFI pulse. Thus, the channel output is independent of the channel input during the RFI pulse. This type of RFI can be modeled as a binary symmetric channel (BSC) with crossover probability of 1/2. When an RFI pulse is present, the overall channel is then a cascade of the BSC and the AWGN channel. This channel is called the RFI/burst saturation channel and represents the worst case RFI/burst channel. It is shown in block diagram form in Figure 2. When an RFI pulse is not present, the channel is simply an AWGN channel.

In the second model, it is assumed that RFI pulses can be detected and the satellite saturation then prevented or blanked. In this case, the RFI can be modeled as a binary erasure channel (BEC) with an erasure probability of 1. When an RFI pulse is present, the overall channel is then a cascade of the BEC and the AWGN channel. This channel is called the RFI/burst blank channel and represents the best case of the RFI/burst channel. It is shown in block diagram form in Figure 3. When an RFI pulse is not present, the channel is simply an AWGN channel.

3 Simulation Results

For the simulations performed in this study, the channel interleaver and RFI/burst channels were not simulated directly. Instead, empirical data obtained from NASA was used to model the combined convolutional interleaver and channel. This was done in order to address specific questions concerning the performance of the system shown in Figure 1. It is a simple matter to simulate the interleaver and channel in a more direct manner.

The empirical data showed that an RFI pulse with a length of approximately 240 consecutive channel symbols resulted in 1 in 15 symbols out of the convolutional deinterleaver being corrupted by the RFI channel. Similarly, an RFI pulse with a length of approximately 360 consecutive channel symbols resulted in 1 in 10 symbols out of the convolutional deinterleaver being corrupted by the RFI channel. Using these observations, the interleaver, RFI/burst channel, and deinteleaver were combined into a single superchannel consisting of an AWGN channel in cascade with a periodic RFI/burst channel. Thus, to simulate the 240 symbol and 360 symbol RFI pulses the period of the superchannel was set to 15 and 10, respectively. The RFI/burst saturation model and the RFI/burst blank model were both used as the periodic RFI/burst channel.

Figure 4 shows the simulated bit error rate (BER) performance of the (2,1,6) convolutional code on the RFI/burst blank superchannel compared to simulation results of the (2,1,6) code on a pure AWGN channel. Decoder truncation lengths of $\tau = 30$ branches and $\tau = 26$ branches were considered.

The RFI/burst superchannel with a period of 15 symbols resulted in a loss of ≈ 0.5dB at a BER of 10^{-5} compared to the AWGN results. A period of 10 symbols resulted in a loss of ≈ 0.8dB at a BER of 10^{-5}. Changing the truncation length had virtually no consequences on the performance of the (2,1,6) code on the RFI/burst blank channel *relative* to the performance on the AWGN channel.

If the (2,1,6) code and the system of Figure 1 are to be used in a concatenated system, the SER performance out of the inner docoder is more significant than the BER. Figure 5 shows the simulated 8-bit symbol error rate (SER) performance of the (2,1,6) code under the same channel conditions that were used in Figure 4. Eight bit symbols were used in order to be compatible with the standard (255,223) Reed-Solomon outer code. The SER performance of the (2,1,6) code degrades in the same manner as the BER.

Figure 6 shows the simulated bit error rate (BER) performance of the (2,1,6) code on the RFI/burst saturation superchannel compared to simulation results of the (2,1,6) code on a pure AWGN channel. As expected, the saturation channel is much more destructive than the blanking channel. With a decoder truncation length of $\tau = 30$, a period of 15 symbols resulted in a loss of ≈ 3.7dB at a BER of 10^{-5}. However, with a decoder truncation length of $\tau = 26$, a period of 15 symbols resulted in a loss of ≈ 4.4dB. The effect of the decoder truncation length was even more significant on the RFI/burst saturation channel when the period was 10 symbols. In this case, there was a loss of ≈ 6.2dB with $\tau = 30$ and a loss of ≈ 8.2dB with $\tau = 26$. Thus, reducing the truncation length caused a performance loss of 2.0dB!

In Figure 7 the 8-bit SER performance is shown under the same channel conditions that were used in Figure 6. The SER performance degrades in the same manner as the BER. In particular, the truncation length has a significant effect on performance.

4 Conclusions

The simulation results in this report are consistent with the analytical results in [1]. The RFI/burst channel is significantly worse than a pure AWGN channel. It is also clear that the ability to detect and blank RFI pulses greatly enhances performance.

It is unclear at this point why the performance of the (2,1,6) code on the RFI/burst saturation is so sensitive to the decoder truncation length. Simulation results for the AWGN channel, shown in Figure 8, demonstrate that the performance of the (2,1,6) code is fairly robust even with a truncation lenth of $\tau = 24$. When the truncation length is reduced to $\tau = 18$, the performance is reduced considerably, but still does not exhibit the divergent behavior evident on the RFI/burst saturation channel. The cause of this phenomenon is currently being investigated.

References

[1] J. P. Odenwalder and A. J. Viterbi, "Final Report on RFI/Coding Sensitivity Analysis for Tracking and Data Relay Satellite System (TDRSS)," Technical Report to ORI, Inc., 13 July 1978.

[2] J. L. Ramsey, "Realization of Optimum Interleavers," *IEEE Trans. on Information Theory*, **IT-16**, pp. 338–345, May 1970.

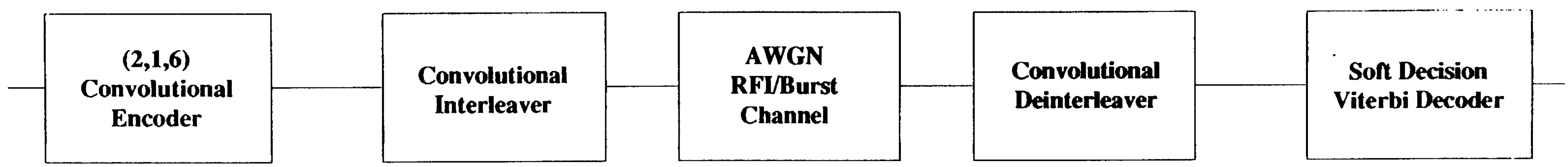

Figure 1: System Model with the (2,1,6) Convolutional Code

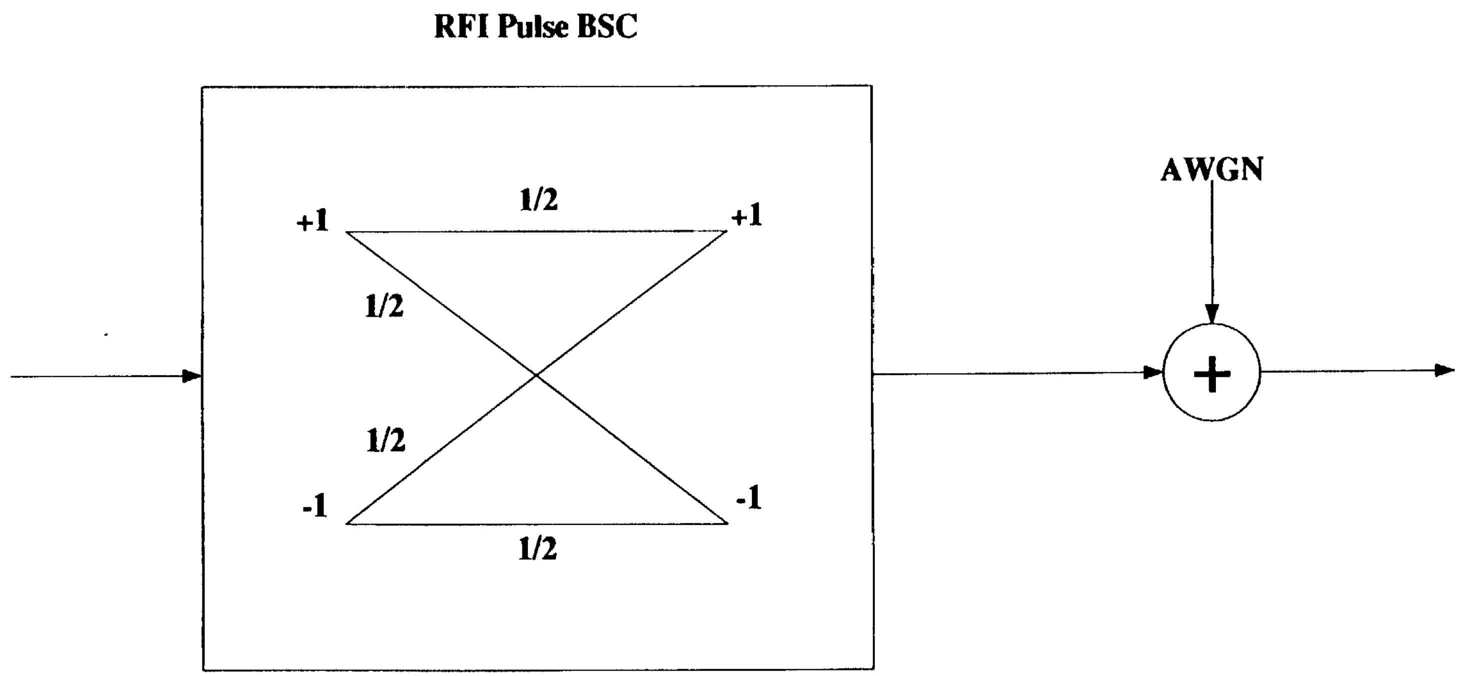

Figure 2: RFI/ Burst Saturation Channel Model

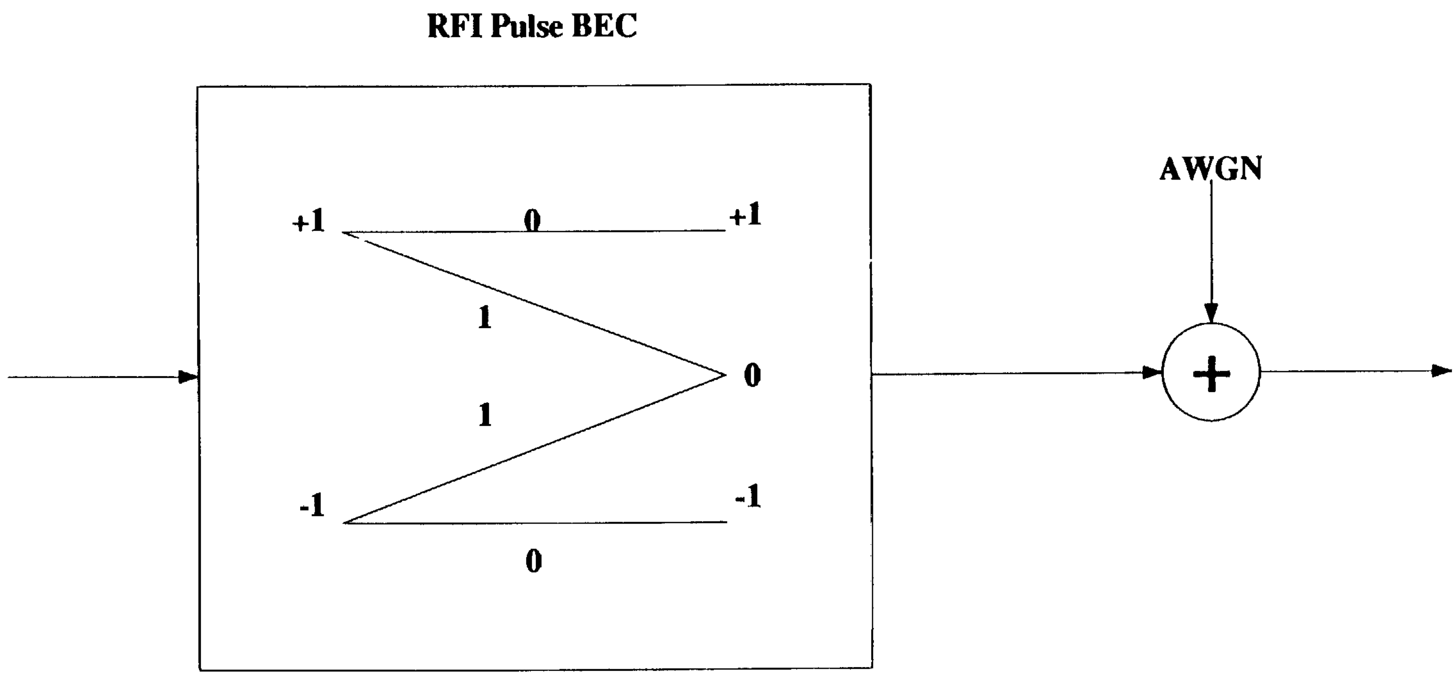

Figure 3: RFI/ Burst Blank Channel Model

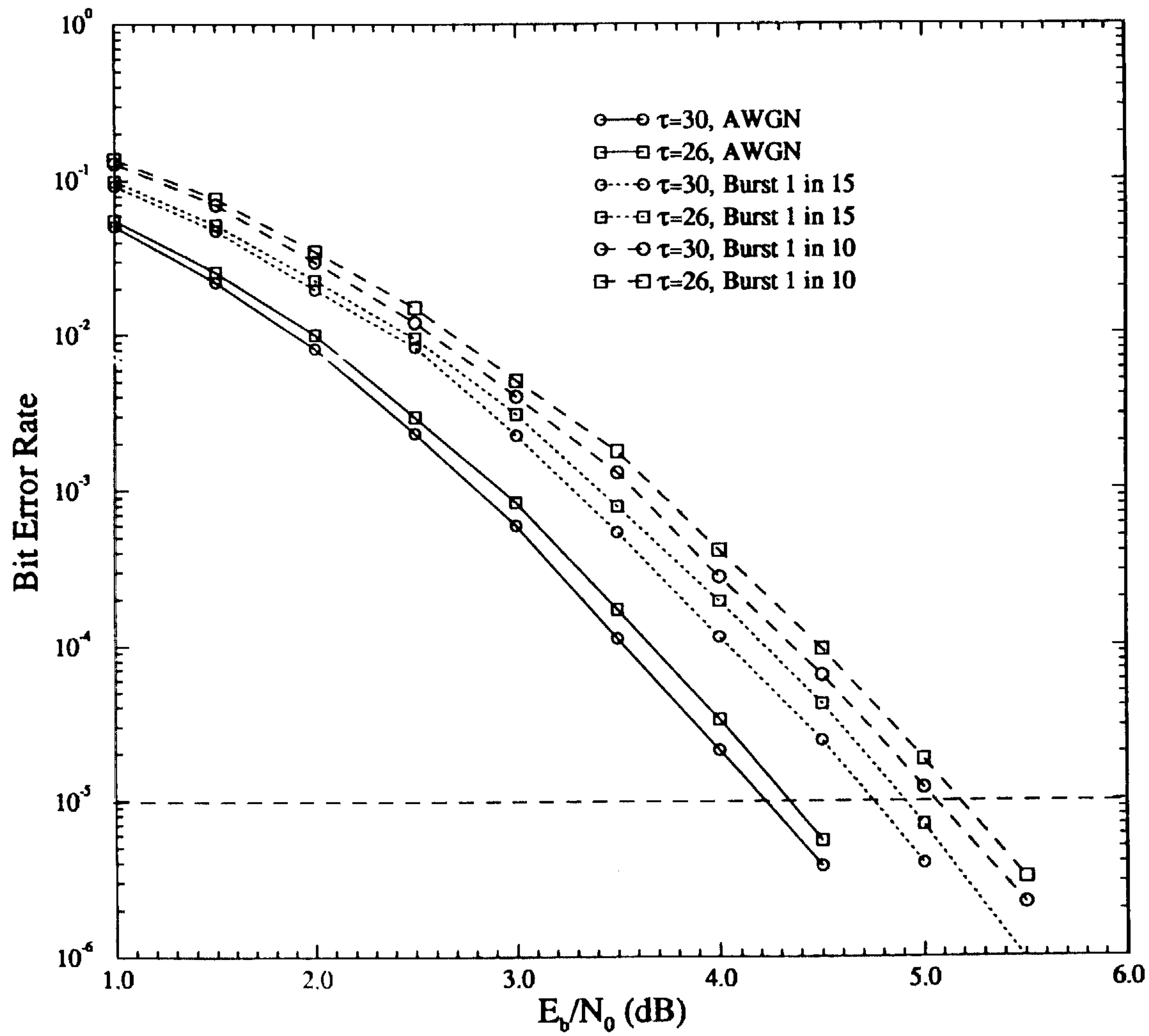

Figure 4: BER Performance of the (2,1,6) Convolutional Code on the RFI/Burst Blank Channel

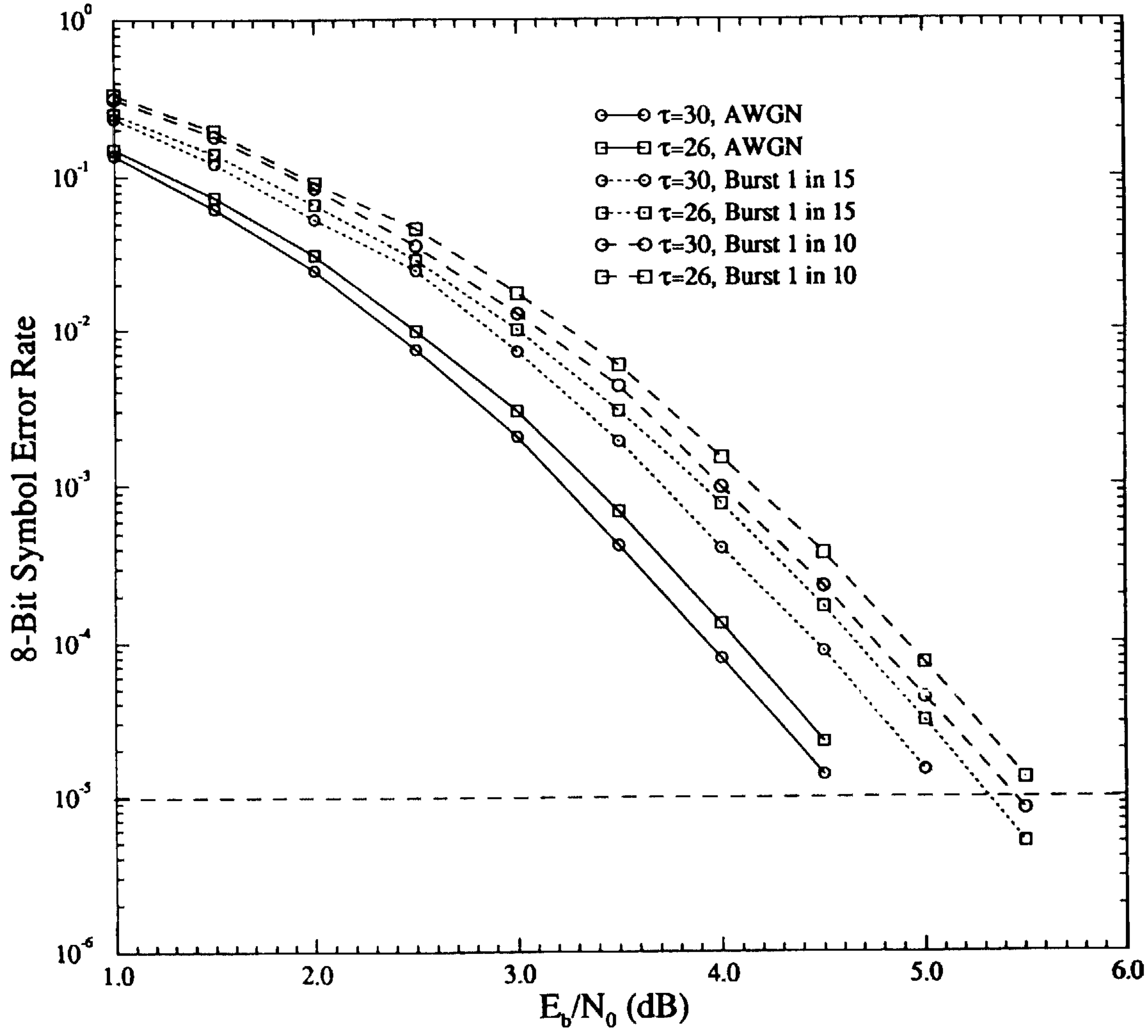

Figure 5: SER Performance of the (2,1,6) Convolutional Code on the RFI/Burst Blank Channel

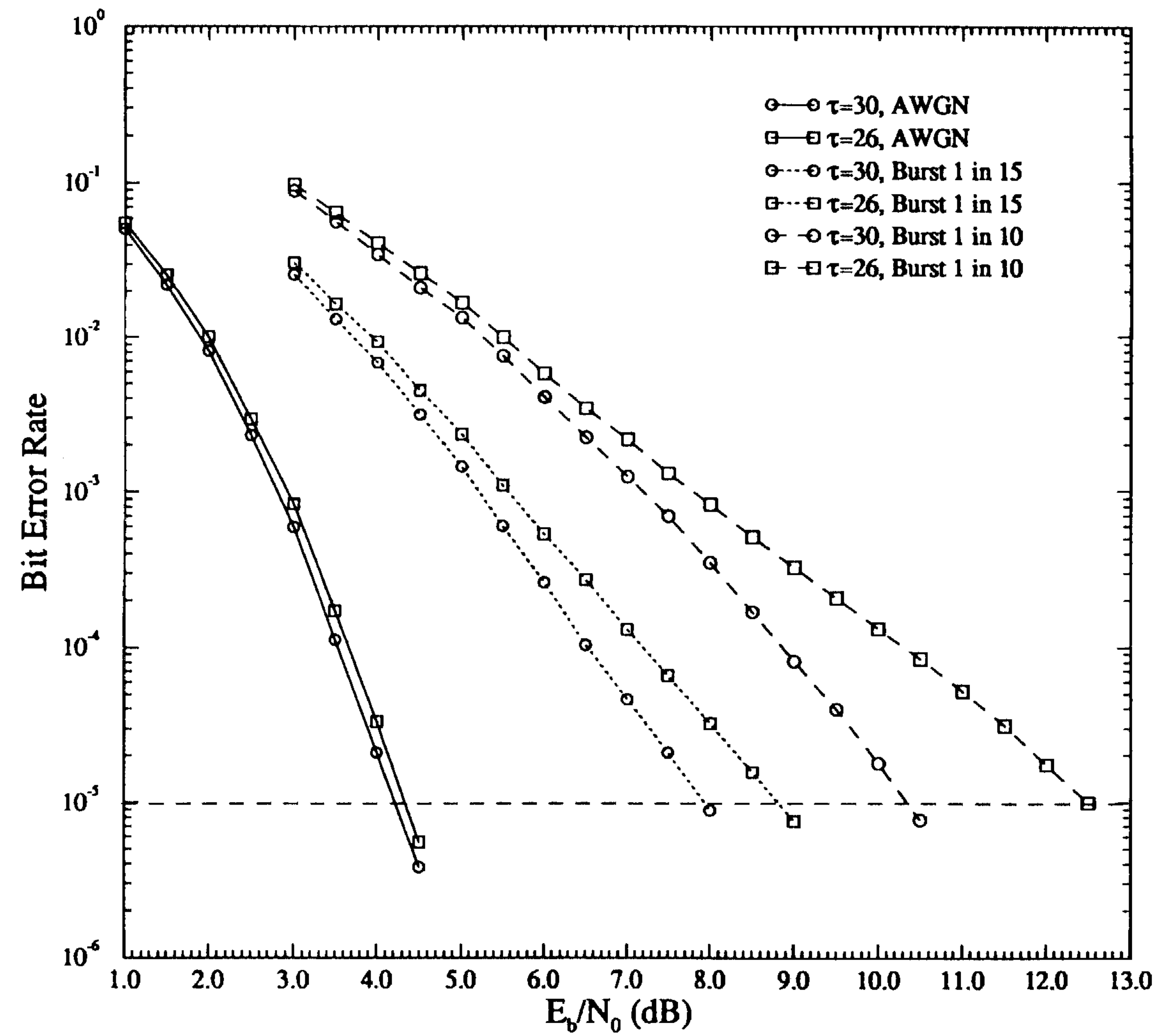

Figure 6: BER Performance of the (2,1,6) Convolutional Code on the RFI/Burst Saturation Channel

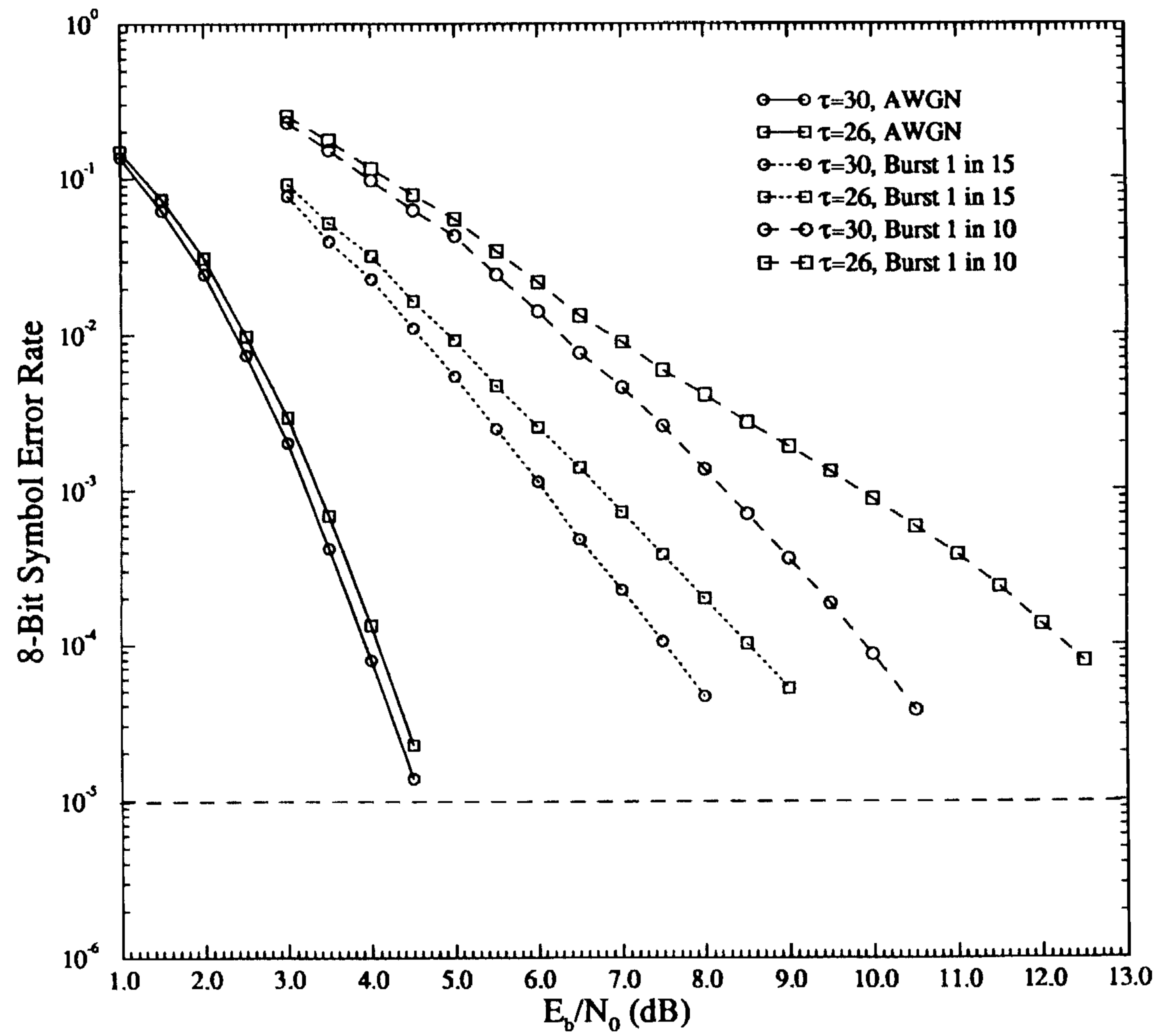

Figure 7: SER Performance of the (2,1,6) Convolutional Code on the RFI/Burst Saturation Channel

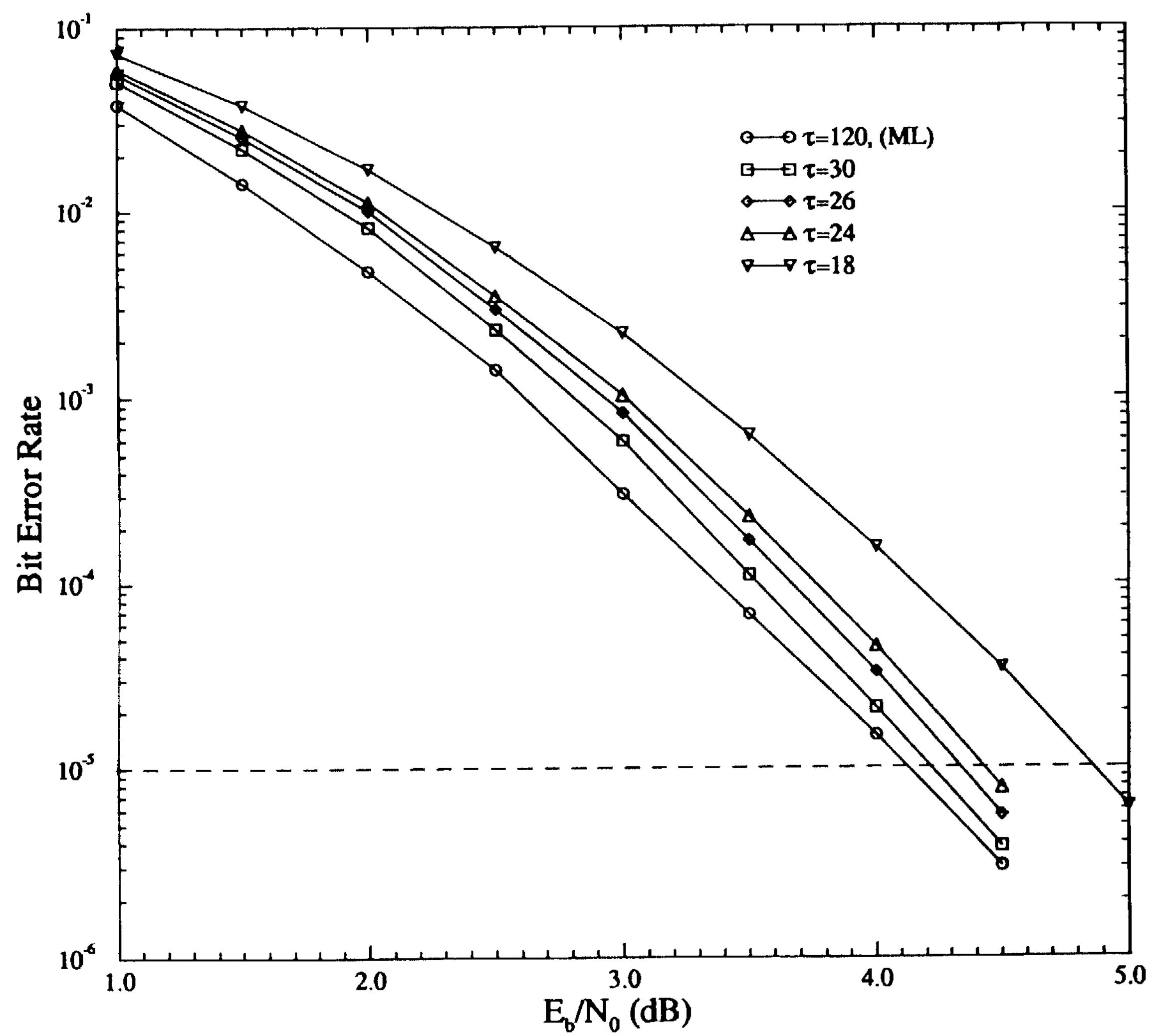

Figure 8: BER Performance of the (2,1,6) Convolutional Code on the AWGN Channel with Varying Truncation Length